

---

# Model-Based Reinforcement Learning for Sepsis Treatment

---

**Aniruddh Raghu**  
MIT  
Cambridge, MA  
araghu@mit.edu

**Matthieu Komorowski**  
Imperial College  
London, United Kingdom  
matthieu.komorowski@gmail.com

**Sumeetpal Singh**  
Cambridge University  
Cambridge, United Kingdom  
sss40@cam.ac.uk

## Abstract

Sepsis is a dangerous condition that is a leading cause of patient mortality. Treating sepsis is highly challenging, because individual patients respond very differently to medical interventions and there is no universally agreed-upon treatment for sepsis. In this work, we explore the use of continuous state-space model-based reinforcement learning (RL) to discover high-quality treatment policies for sepsis patients. Our quantitative evaluation reveals that by blending the treatment strategy discovered with RL with what clinicians follow, we can obtain improved policies, potentially allowing for better medical treatment for sepsis.

## 1 Introduction

Sepsis (severe infections with organ failure) is a dangerous condition that is a leading causing of patient mortality and is expensive for hospitals to treat [1, 20]. Sepsis is often managed by giving patients intravenous fluids and vasopressors. Different dosage strategies for these two interventions can greatly affect patient outcomes, which demonstrates how important treatment decisions are [21]. However, clinicians still lack decision support tools to assist them when treating patients with sepsis [17]. This work explores the use of reinforcement learning (RL) to provide medical decision support for sepsis treatment, developing on earlier research [10, 14]. We consider the use of continuous state-space model-based RL algorithms and observational data from intensive care units (ICUs) to deduce medical treatment strategies (or *policies*) for sepsis. We demonstrate how blending our learned policies with what clinicians follow could lead to better medical treatment for sepsis.

## 2 Preliminaries

**Reinforcement Learning (RL):** In the RL problem, an agent’s interaction with an environment can be represented by a Markov Decision Process (MDP). At every timestep  $t$ , an agent observes the current state of the environment  $s_t$ , takes an action  $a_t$  according to a *policy*,  $\pi(a_t|s_t)$ , receives a reward  $r_t$ , and transitions to a new state  $s_{t+1}$  with probability  $P(s_{t+1}|s_t, a_t)$ , where  $P$  is the transition probability distribution. The *return* is defined as  $R_{0:T-1} = \sum_{t=0}^{T-1} \gamma^t r_t$ , where  $\gamma$  captures the tradeoff between immediate and future rewards, and  $T$  is the terminal timestep. The value of a policy  $\pi$ ,  $V^\pi$ , represents its quality, and is defined as the expected return over trajectories  $\{H_i\}$  it generates:  $V^\pi = \mathbb{E}_{H \sim P_\pi} [R_{0:T-1}(H)]$ . We consider continuous state-space model-based RL, where we model the transition distribution  $P$  and then using this to find a good-quality policy  $\pi$ . Prior work has considered model-free RL [14], and discrete state-space model-based RL [10].

**Related work:** RL has previously been used in healthcare settings. Sepsis treatment strategy was tackled by [10], where model-based RL with discretized state and action-spaces were used to deduce treatment policies. [14] extended this work to consider continuous state-space model-free RL. In

our work, we build on both approaches: we explore the use of continuous state-space model-based RL, which is challenging due to having to model the transition distribution of the MDP, but also potentially more data-efficient. We also extend our quantitative evaluation based on recent work [16].

**Data and preprocessing:** In this work, we consider a cohort of patients from the Medical Information Mart for Intensive Care (MIMIC-III v1.4) database [8] fulfilling the Sepsis-3 criteria [19] (17,898 in total), as in [14]. For each patient, we have relevant physiological parameters including demographics, lab values, vital signs, and intake/output events, discretized into 4 hour timesteps. In order to capture temporal patterns in a patient’s physiology, the state representation used in this work concatenates the previous three timesteps’ raw state information to the current time’s state vector, resulting in a vector of length 198, which is the state  $s_t$  in the underlying MDP. See Section 6.3 for the full list of features used at each timestep.

**Actions and rewards:** We define a  $5 \times 5$  action space for the medical interventions, as in [14] covering dosages of intravenous (IV) fluid (volume adjusted for fluid tonicity) and maximum vasopressor (VP) dosage in a given 4 hour window. More information is provided in Section 6.4. The reward function follows from [14], and is clinically guided: positive rewards are issued at intermediate timesteps for improvements in a patient’s wellbeing (with improvement being defined by reductions in severity scores, such as SOFA), and negative rewards for deterioration. At the terminal timestep of a patient’s trajectory, a reward is assigned that is positive in the case of survival, and negative otherwise. See Section 6.5 for more information.

### 3 Model-based RL

We now explore our model-based RL approach to learning sepsis treatment strategies.

#### 3.1 Environment modelling

We first construct a model to represent the transition dynamics of the underlying MDP, which we address by learning an environment model. This framing of the problem is motivated by the discussion in Nagabandi et al. [13]. We consider the task of predicting  $\Delta_t = s_{t+1} - s_t$ , the change in a patient’s physiological state, which is achieved by learning a function  $f(h_t; \theta)$  where:  $\Delta_t = f(h_t; \theta) + \epsilon$ ;  $\epsilon \sim \mathcal{N}(\mathbf{0}, \mathbf{I})$ , and  $h_t = g(s_t, a_t, s_{t-1}, a_{t-1}, \dots)$ .

The function  $g$  concatenates the current state-action pair  $(s_t, a_t)$  with the previous three timesteps’ state-action pairs. This is to capture some amount of historical information about the patient’s physiology. Cross-validation performance (in terms of prediction mean squared error) motivated the use of three past timesteps of information.

We considered several different environment models:

- Linear regression to predict  $\Delta_t$
- Neural network: the best architecture had two fully connected layers with ReLU activations, and batch normalization [7] after each layer. This was trained using Adam [9].
- Recurrent neural network (RNN); specifically, an LSTM [6]. This was trained using Adam [9].
- Bayesian neural network (BNN): this is advantageous as it can represent the full predictive distribution over  $\hat{\Delta}_t$  instead of providing point estimates. We based our BNN modelling approach on that of [2]. The best BNN had two hidden layers, each with 32 hidden units and tanh nonlinearities, and was implemented using the Autograd library [12]. A full description of BNN modelling is provided in Section 6.6.

**Results:** Table 1 shows the mean squared error (MSE) when predicting  $\Delta_t$  when using different environment models: Linear Regression (LR), feedforward Neural Network (NN), Recurrent Neural Network (RNN), and Bayesian Neural Network (BNN).

The RNN obtains the best MSE by this metric. Analysis reveals that this is because the predictions produced by the RNN at large timesteps are very accurate. However, the performance of the RNN at small values of  $t$  are poor; the RNN does not have the capacity to predict  $\Delta_t$  accurately at small  $t$ . The feedforward neural network is therefore preferred as an environment model.

Table 1: Mean squared error (MSE) on a held-out validation set when predicting  $\Delta_t$  for different environment models: Linear Regression (LR), feedforward Neural Network (NN), Recurrent Neural Network (RNN), and Bayesian Neural Network (BNN).

	LR	NN	RNN	BNN
MSE	0.195	0.171	<b>0.122</b>	0.220

Figure 1 shows some examples of rollouts for the SOFA score using the neural network as an environment model, using the first state in a trajectory and clinician actions at subsequent timesteps. The neural network can sometimes represent the overall trend in SOFA score over a patient’s trajectory accurately; this is most noticeable for Figures 1a, 1b. This task is however very challenging – there are large changes in the value of the SOFA score at certain timesteps, and there are timesteps where the values do not change at all. The accuracy of the predictions worsens as we increase the length of the rollout. The modelling performance is not perfect, but given that the model can capture the overall SOFA trend, it may be sufficiently accurate to aid in discovering improved policies. However, further work is necessary on this task.

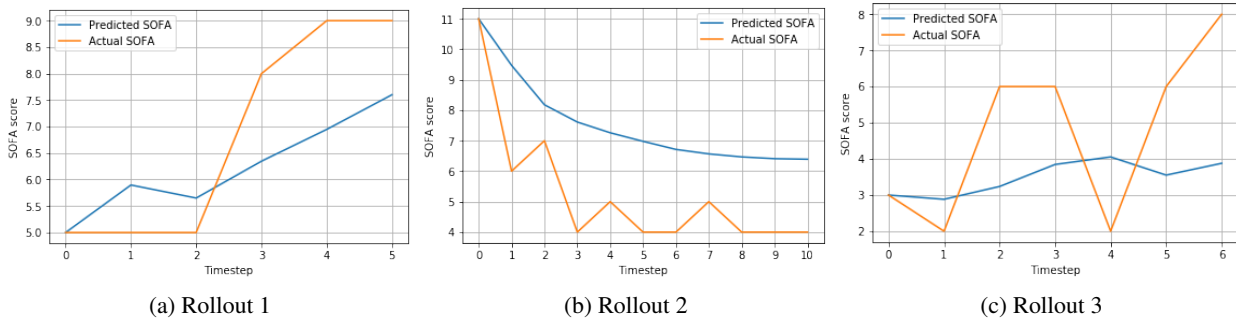


Figure 1: Rollouts from the neural network environment model for the SOFA score, an important physiological feature. Predictions from the network can approximately capture the trend in SOFA score in certain cases, but not others.

### 3.2 Policy search

After learning an environment model, policy search algorithms are used to find an appropriate policy  $\pi$ . It is important not to stray too far from the policy used by clinicians for interpretability reasons; therefore, the approach to discover improved treatment strategies proceeded as follows:

- Learn the parameters  $\phi$  describing the clinician policy,  $\mu(a|h_t; \phi)$ , using supervised learning.
- Initialise the parameters  $\theta$  of a new policy  $\pi(a|h_t; \theta)$  using  $\phi$ .
- Using the learned environment model, simulate rollouts from  $\pi(a|h_t; \theta)$ . Use a policy improvement algorithm with a small learning rate (to stay close to  $\mu$ ) to improve  $\pi$ .

**Modelling clinician behaviour:** We formulated learning the clinician policy  $\mu$  as a behaviour cloning task, where we learned parameters  $\phi^*$  that minimised the average cross-entropy between the predictive distribution over actions from the neural network and the label distribution (encoding the action taken by the clinician). The best-performing model was a two-layer feedforward neural network with 64 hidden units in each layer, with ReLU activations. An L2 regularisation penalty was added to the loss to prevent overfitting.

**Policy improvement:** To improve  $\pi$ , we compare the performance of two policy improvement algorithms: the REINFORCE Policy Gradient algorithm (PG) [22], and the Proximal Policy Optimization algorithm (PPO) [18]. Our procedure firstly involves sampling a random trajectory from the dataset, to get a starting state. We then perform a rollout from this starting state for 10 timesteps, using actions sampled from  $\pi(a|h_t; \theta)$ . We use the policy improvement algorithms with these trajectories to improve  $\pi$ .

### 3.3 Evaluation of learned policies

Qualitative analysis of learned treatment policies (as seen in previous work by [15]) does not necessarily provide an absolute indicator of performance, explored in more detail by [4]. We therefore consider quantitative evaluation of learned policies, using Off-Policy Policy Evaluation (OPE). Our evaluation uses the Per-Horizon Weighted Importance Sampling (PHWIS), Per-Horizon Weighted Doubly Robust (PHWDR), and Approximate Model (AM) estimators, discussed in [16]. We follow the suggestions of [16] when constructing these estimators. To model the clinical policy (behaviour policy) for these estimators, an approximate k-Nearest Neighbours (kNN) model with  $k = 250$  was used. To obtain the AM estimator and the AM terms for the PHWDR estimator, the Fitted Q Iteration (FQI) algorithm [3] was used with a random forest with 80 trees. We do not use recent model-based estimators, introduced by [11], because of the challenge in learning full environment models in this domain.

We present results here for the PPO algorithm; the PG algorithm performed relatively poorly in comparison. We also consider blending the clinician’s policy and the RL algorithm’s policy in different severity regimes (deduced by SOFA score); the environment model is not as accurate in high and low severity regimes (due to high stochasticity and less signal respectively). Given the safety-critical nature of this domain, we rely on the clinician’s policy in regimes where the model has inferior performance. For comparison, note that the value of the clinician’s policy,  $V^{\pi_b}$ , obtained by averaging returns in the dataset, is found to be 9.90. The policy evaluated is denoted  $\pi_e$ .

Table 2 presents results using the PHWIS, PHWDR, and AM estimators. These results show that the AM estimator does not appear to discriminate significantly between the learned policies; all policies have similar values. When considering the PHWIS and PHWDR estimators, it appears that the best policy is obtained when relying on the clinical policy in the low and high severity regimes, and the RL-learned policy in the medium severity regime. The two estimation procedures show reasonable agreement in estimated value, though there are discrepancies between them. However, as both show similar trends, it may be possible to conclude that this policy does improve on what clinicians currently follow. Investigating the specific policy discovered in this regime could offer valuable clinical insight. The result obtained can also be interpreted – in low/high severity regimes, clinicians may have a set protocol they follow, which performs well; it therefore does not make sense to deviate from this. In the medium severity regime, there is more variability in clinician action, and model-based RL is effective in identifying suitable courses of action.

Table 2: OPE results using the PHWIS, PHWDR, and AM estimators when relying on combinations of the clinician’s policy and the PPO policy. Results are also shown for following the clinical policy in all regimes. By relying on the clinician policy in regimes where the environment model is weaker, improvements in performance are observed for the PHWIS and PHWDR estimators.

Low SOFA	Medium SOFA	High SOFA	$\hat{V}_{\text{PHWIS}}^{\pi_e}$	$\hat{V}_{\text{PHWDR}}^{\pi_e}$	$\hat{V}_{\text{AM}}^{\pi_e}$
PPO	PPO	PPO	10.8	11.5	9.33
PPO	PPO	Clinician	11.7	11.8	9.35
Clinician	PPO	Clinician	<b>12.1</b>	<b>12.8</b>	9.35
PPO	Clinician	PPO	7.63	7.58	9.34
Clinician	Clinician	Clinician	10.2	9.87	<b>9.36</b>

## 4 Conclusions

In this work, we proposed a method to learn medical treatment strategies for sepsis with model-based reinforcement learning. We used a neural network to model physiological dynamics, and demonstrated how to learn treatment policies using a behavioural cloning objective and policy improvement algorithms (Proximal Policy Optimisation). Our quantitative evaluation revealed we could find potentially improved treatment strategies by blending clinical and RL-learned policies, which could lead to improved treatment for sepsis patients.

## 5 Acknowledgements

The authors would like to thank Omer Gottesman, Yao Liu, Finale Doshi-Velez, and Emma Brunskill for helpful comments and suggestions.

## References

- [1] J. Cohen, J.-L. Vincent, N. K. J. Adhikari, F. R. Machado, D. C. Angus, T. Calandra, K. Jaton, S. Giulieri, J. Delaloye, S. Opal, K. Tracey, T. van der Poll, and E. Pelfrene. Sepsis: a roadmap for future research. *Lancet Infectious Diseases*, 15(5):581–614, 2006.
- [2] Stefan Depeweg, José Miguel Hernández-Lobato, Finale Doshi-Velez, and Steffen Udluft. Learning and policy search in stochastic dynamical systems with Bayesian neural networks. *arXiv preprint arXiv:1605.07127*, 2016.
- [3] Damien Ernst, Pierre Geurts, and Louis Wehenkel. Tree-based batch mode reinforcement learning. *Journal of Machine Learning Research*, 6(4):503–556, 2005.
- [4] Omer Gottesman, Fredrik Johansson, Joshua Meier, Jack Dent, Donghun Lee, Srivatsan Srinivasan, Linying Zhang, Yi Ding, David Wihl, Xuefeng Peng, et al. Evaluating reinforcement learning algorithms in observational health settings. *arXiv preprint arXiv:1805.12298*, 2018.
- [5] Jose Hernandez-Lobato, Yingzhen Li, Mark Rowland, Thang Bui, Daniel Hernandez-Lobato, and Richard Turner. Black-box alpha divergence minimization. In *International Conference on Machine Learning*, pages 1511–1520, 2016.
- [6] Sepp Hochreiter and Jürgen Schmidhuber. Long short-term memory. *Neural computation*, 9(8):1735–1780, 1997.
- [7] Sergey Ioffe and Christian Szegedy. Batch normalization: Accelerating deep network training by reducing internal covariate shift. In *International Conference on Machine Learning*, pages 448–456, 2015.
- [8] A. E. W. Johnson, T. J. Pollard, L. Shen, L.-W. H. Lehman, M. Feng, M. Ghassemi, B. Moody, P. Szolovits, L. Anthony Celi, and R. G. Mark. MIMIC-III, a freely accessible critical care database. *Scientific Data*, 4(160035):122, 2016.
- [9] Diederik P Kingma and Jimmy Ba. Adam: A method for stochastic optimization. *arXiv preprint arXiv:1412.6980*, 2014.
- [10] M. Komorowski, A. Gordon, L. A. Celi, and A. Faisal. A Markov Decision Process to suggest optimal treatment of severe infections in intensive care. In *Neural Information Processing Systems Workshop on Machine Learning for Health*, December 2016.
- [11] Yao Liu, Omer Gottesman, Aniruddh Raghu, Matthieu Komorowski, Aldo Faisal, Finale Doshi-Velez, and Emma Brunskill. Representation balancing mdps for off-policy policy evaluation. *arXiv preprint arXiv:1805.09044*, 2018.
- [12] Dougal Maclaurin, David Duvenaud, and Matthew Johnson. Autograd. URL <https://github.com/HIPS/autograd>. Accessed 21 May 2018.
- [13] Anusha Nagabandi, Gregory Kahn, Ronald S Fearing, and Sergey Levine. Neural network dynamics for model-based deep reinforcement learning with model-free fine-tuning. *arXiv preprint arXiv:1708.02596*, 2017.
- [14] Aniruddh Raghu, Matthieu Komorowski, Imran Ahmed, Leo Celi, Peter Szolovits, and Marzyeh Ghassemi. Deep reinforcement learning for sepsis treatment. *arXiv preprint arXiv:1711.09602*, 2017.
- [15] Aniruddh Raghu, Matthieu Komorowski, Leo Anthony Celi, Peter Szolovits, and Marzyeh Ghassemi. Continuous state-space models for optimal sepsis treatment: a deep reinforcement learning approach. In *Machine Learning for Healthcare Conference*, pages 147–163, 2017.
- [16] Aniruddh Raghu, Omer Gottesman, Yao Liu, Matthieu Komorowski, Aldo Faisal, Finale Doshi-Velez, and Emma Brunskill. Behaviour policy estimation in off-policy policy evaluation: Calibration matters. *arXiv preprint arXiv:1807.01066*, 2018.
- [17] Andrew Rhodes, Laura E Evans, Waleed Alhazzani, Mitchell M Levy, Massimo Antonelli, Ricard Ferrer, Anand Kumar, Jonathan E Sevransky, Charles L Sprung, Mark E Nunnally, et al.

- Surviving sepsis campaign: International guidelines for management of sepsis and septic shock: 2016. *Intensive care medicine*, 43(3):304–377, 2017.
- [18] John Schulman, Filip Wolski, Prafulla Dhariwal, Alec Radford, and Oleg Klimov. Proximal policy optimization algorithms. *arXiv preprint arXiv:1707.06347*, 2017.
- [19] M. Singer, C. S. Deutschman, C. Seymour, et al. The third international consensus definitions for sepsis and septic shock (sepsis-3). *JAMA*, 315(8):801–810, 2016. doi: 10.1001/jama.2016.0287. URL <http://dx.doi.org/10.1001/jama.2016.0287>.
- [20] J.-L. Vincent, Y. Sakr, C. L. Sprung, V. M. Ranieri, K. Reinhart, H. Gerlach, R. Moreno, J. Carlet, J.-R. Le Gall, and D. Payen. Sepsis in European intensive care units: results of the SOAP study. *Critical Care Medicine*, 34(2):344–353, 2006.
- [21] Jason Waechter, Anand Kumar, Stephen E Lapinsky, John Marshall, Peter Dodek, Yaseen Arabi, Joseph E Parrillo, R Phillip Dellinger, Allan Garland, and Cooperative Antimicrobial Therapy of Septic Shock Database Research Group and others. Interaction between fluids and vasoactive agents on mortality in septic shock: a multicenter, observational study. *Critical care medicine*, 42(10):2158–2168, 2014.
- [22] Ronald J Williams. Simple statistical gradient-following algorithms for connectionist reinforcement learning. In *Reinforcement Learning*, pages 5–32. Springer, 1992.

## 6 Appendix

### 6.1 Cohort definition

Following the latest guidelines, sepsis was defined as a suspected infection (prescription of antibiotics and sampling of bodily fluids for microbiological culture) combined with evidence of organ dysfunction, defined by a Sequential Organ Failure Assessment (SOFA) score greater or equal to 2 [19]. We assumed a baseline SOFA of zero for all patients. For cohort definition, we respected the temporal criteria for diagnosis of sepsis: when the microbiological sampling occurred first, the antibiotic must have been administered within 72 hours, and when the antibiotic was given first, the microbiological sample must have been collected within 24 hours [19]. The earliest event defined the onset of sepsis. We excluded patients who received no intravenous fluid, and those with missing data for 8 or more out of the 48 variables. This method yield a cohort of 17,898 patients.

The resulting cohort is described in Table 3.

Table 3: Summary statistics for the patient cohort.

	% Female	Mean Age	Hours in ICU	Total Population
Survivors	43.6	63.4	57.6	15,583
Non-survivors	47.0	69.9	58.8	2,315

### 6.2 Data extraction

MIMIC-III v1.4 was queried using pgAdmin 4. Raw data were extracted for all 47 features and processed in Matlab (version 2016b). Data were included from up to 24 hours preceding the diagnosis of sepsis and until 48 hours following the onset of sepsis, in order to capture the early phase of its management including initial resuscitation, which is the time period of interest. The features were converted into multidimensional time series with a time resolution of 4 hours. The outcome of interest was in-hospital mortality.

### 6.3 Model Features

**Choice of features:** the included features were chosen to represent the most important parameters clinicians would examine when deciding treatment and dosage for patients; however, some factors not included in our feature vector could serve as confounding factors. Exploring the effect of these is an important future direction.

The physiological features used in our model are:

**Demographics/Static:** Shock Index, Elixhauser, SIRS, Gender, Re-admission, GCS - Glasgow Coma Scale, SOFA - Sequential Organ Failure Assessment, Age

**Lab Values:** Albumin, Arterial pH, Calcium, Glucose, Hemoglobin, Magnesium, PTT - Partial Thromboplastin Time, Potassium, SGPT - Serum Glutamic-Pyruvic Transaminase, Arterial Blood Gas, BUN - Blood Urea Nitrogen, Chloride, Bicarbonate, INR - International Normalized Ratio, Sodium, Arterial Lactate, CO<sub>2</sub>, Creatinine, Ionised Calcium, PT - Prothrombin Time, Platelets Count, SGOT - Serum Glutamic-Oxaloacetic Transaminase, Total bilirubin, White Blood Cell Count

**Vital Signs:** Diastolic Blood Pressure, Systolic Blood Pressure, Mean Blood Pressure, PaCO<sub>2</sub>, PaO<sub>2</sub>, FiO<sub>2</sub>, PaO/FiO<sub>2</sub> ratio, Respiratory Rate, Temperature (Celsius), Weight (kg), Heart Rate, SpO<sub>2</sub>

**Intake and Output Events:** Fluid Output - 4 hourly period, Total Fluid Output, Mechanical Ventilation

**Miscellaneous:** Timestep

## 6.4 Action space

We discretized the action space into per-drug quartiles based on all non-zero dosages of the two drugs, and converted each drug at every timestep into an integer representing its quartile bin. We included a special case of no drug given as bin 0. This created an action representation of interventions as tuples of (total IV in, max VP in) at each time. We choose to focus on this action space given the uncertainty in clinical literature of how to adjust these interventions on a per-patient basis, and also their crucial impact on a patient’s eventual outcome [21].

## 6.5 Reward function

As our objective is to improve patient survival, the model should receive a reward when the patient’s state improves, and a penalty when the patient’s state deteriorates. This reward should be comprised of the best indicators of patient health; in this situation, these indicators include the patient’s SOFA score (which summarizes the extent of a patient’s organ failure and thus acts as a proxy for patient health) as well as the patient’s lactate levels (a measure of cell-hypoxia that is higher in septic patients because sepsis-induced low blood pressure reduces oxygen perfusion into tissue). An effective reward function should penalize high SOFA scores as well as increases in SOFA score and reward decreases in SOFA scores between states. Similarly, for lactate, increases in lactate should be penalized while decreases in lactate should be rewarded.

We opted for a reward function for intermediate timesteps as follows:

$$r(s_t, s_{t+1}) = C_0 \mathbb{1}(s_{t+1}^{\text{SOFA}} = s_t^{\text{SOFA}} \ \& \ s_{t+1}^{\text{SOFA}} > 0) + C_1 (s_{t+1}^{\text{SOFA}} - s_t^{\text{SOFA}}) + C_2 \tanh(s_{t+1}^{\text{Lactate}} - s_t^{\text{Lactate}})$$

We experimented with multiple parameters and opted to use  $C_0 = -0.025$ ,  $C_1 = -0.125$ ,  $C_2 = -2$ .

At terminal timesteps, we issue a reward of +15 if a patient survived their ICU stay, and a negative reward of -15 if they did not.

The reason behind the chosen parameters for the intermediate reward, as well as the form of the equation above, was to ensure that the reward was limited in magnitude and would not eclipse the terminal timestep reward at the end of each patient’s trajectory. This was also the motivation behind using the tanh function when dealing with lactate changes: because the maximum change was significantly higher than the average change between timesteps, we opted to use a tanh to cap the maximum reward/penalty to  $|C_2|$ .

## 6.6 BNN modelling

These models represent the full predictive distribution over  $\hat{\Delta}_t$  instead of providing point estimates.

The description provided here is based on that in Depeweg et al. [2].

As with non-Bayesian neural networks, a likelihood model is specified, mapping the input to the output, using a series of linear transformations and pointwise nonlinearities. A prior distribution is specified over the values of the parameters of the weight matrices and bias vectors; in this case, it is a Gaussian with zero mean and specifiable variance:  $\theta_i \sim \mathcal{N}(0, \sigma_i^2)$ .

In BNN modelling, we aim to form the posterior distribution over the parameters given the training data, consisting of  $(h_t, \Delta_t)$  pairs, and marginalise out the parameters to get the predictive distribution over  $\hat{\Delta}_t$ .

However, as this marginalisation procedure is intractable, we form a variational approximation to the posterior distribution,  $q(\theta|\mathcal{D})$ , and minimise the alpha-divergence between the true posterior and the variational approximation [5]. This minimisation procedure aims to find the parameters of the approximate posterior; that is, the mean and variance of the Gaussian distributions that make up the approximate posterior distribution.

Samples from the predictive distribution are then obtained by sampling parameter values from the approximate posterior and averaging:

$$\begin{aligned} p(\hat{\Delta}_t|h_t, \mathcal{D}) &= \int p(\hat{\Delta}_t|h_t, \mathcal{D}, \theta)q(\theta|\mathcal{D})d\theta \\ &\approx \frac{1}{N} \sum_{i=1}^N p(\hat{\Delta}_t|h_t, \mathcal{D}, \theta_i); \quad \theta_i \sim q(\theta|\mathcal{D}) \end{aligned}$$

The best BNN had two hidden layers, each with 32 hidden units and tanh nonlinearities. It was implemented using the Autograd library [12].